Analytical Methods

Accepted Manuscript

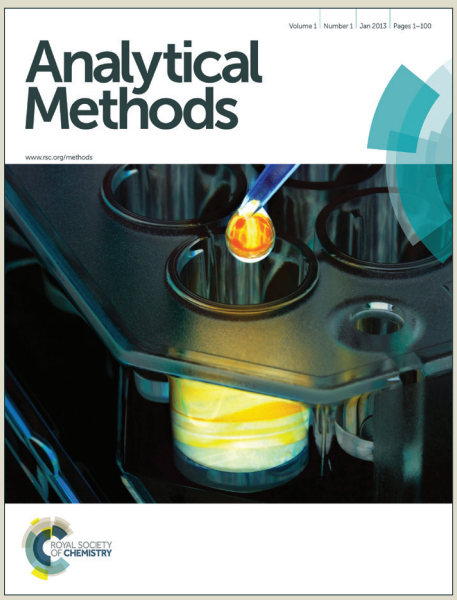

This is an *Accepted Manuscript*, which has been through the Royal Society of Chemistry peer review process and has been accepted for publication.

Accepted Manuscripts are published online shortly after acceptance, before technical editing, formatting and proof reading. Using this free service, authors can make their results available to the community, in citable form, before we publish the edited article. We will replace this *Accepted Manuscript* with the edited and formatted *Advance Article* as soon as it is available.

You can find more information about *Accepted Manuscripts* in the Information for Authors.

ROYAL SOCIETY OF CHEMISTRY

www.rsc.org/methods

Facile Synthesis of Nanosized Graphene/Nafion Hybrid Materials and Its Application in Electrochemical Sensing of Nitric Oxide

Norazriena Yusoff [1], Alagarsamy Pandikumar [1,*], Marlinda Ab Rahman [1], Huang Nay Ming [1,*] and Lim Hong Ngee [2]

[1] Low Dimensional Materials Research Centre, Department of Physics, Faculty of Science, University of Malaya, 50603 Kuala Lumpur, Malaysia.

[2] Department of Chemistry, Faculty of Science, University Putra Malaysia, 43400 UPM Serdang, Selangor Darul Ehsan, Malaysia.

*Corresponding Author(s): pandikumarinbox@gmail.com; huangnayming@um.edu.my

Abstract: This paper presents the preparation of nanosized graphene hybridized with nafion using a simple two step method, sonication and hydrothermal process which successfully produced a new nanosized graphene-nafion hybrid (G-Nf) with lateral dimensions as small as 18 nm based on AFM results. The novel G-Nf hybrids were used to modified glassy carbon electrode (GCE) for the fabrication of nitric oxide (NO) electrochemical sensor where the optimum sensing response was achieved with a G-Nf hybrid synthesized after 16 h of hydrothermal treatment. Under the optimized experimental conditions, the GC/G-Nf (16 h) electrode showed an oxidation peak at 0.85 V in the presence of NO. It also demonstrated an excellent performance toward the detection of NO, with a limit of detection of 11.61 μM (S/N = 3) in a linear range of 0.05–0.45 mM. Moreover, this GC/G-Nf (16 h) electrode exhibited a higher sensitivity of approximately 62 μA mM^{-1} and had a great selectivity toward NO in the presence of interference such as dopamine and ascorbic acid. The combination of nanosized graphene and nafion generate a synergic effect which facilitates excellent electron-transfer processes between the electrolyte and the GCE thus improved the sensing performance of the fabricated modified electrode.

Keywords: Graphene, Nanosized, Nafion, Nitric oxide, Electrochemical sensor.

1. Introduction

Nitric oxide (NO) is a hydrophobic, highly labile free radical that is naturally produced within the human body and plays a vital role in a wide range of biological and cellular functions. NO is used for communication between cells and is involved in the regulation of blood pressure, the immune response, platelet aggregation and clotting, neurotransmission, and possibly respiration [1, 2]. Abnormal NO production and bioavailability may cause several diseases such as obesity, diabetes (both type I and II), atherosclerosis, hypertension, and heart failure [3, 4]. Thus, the development of sensor for the precise and selective measurement of NO at the low levels characteristic of living systems can make a great contribution to disease diagnosis.

A variety of materials have been reported to have potential as electrochemical sensors, including organic conjugated polymer [5, 6], metal and semiconductor nanoparticles [7], and carbon nanomaterials [8]. Among the carbon nanomaterials, graphene has been widely explored for the fabrication of electrochemical sensors, and especially biosensor, because of its fascinating two-dimensional conjugated structures and excellent properties such as a high conductivity [9], high electrocatalytic activity [10], and large surface area [11]. The high surface area of electrically conductive graphene sheets can give rise to high densities of attached analyte molecules. This in turn can facilitate high sensitivity and device miniaturization in biosensor application.

Several methods have been reported to detect NO, including chemiluminescence [12], paramagnetic resonance spectrometry [13], paramagnetic resonance imaging spectrophotometry [14], and bioassay [15]. Among these methods, the electrochemical detection of NO is the only available technique sensitive enough to detect relevant concentrations of NO in real time and

in vivo. Electrochemical biosensor has a series of advantages such as high sensitivity and selectivity towards NO in the presence of interfering species such as nitrite, nitrate, dopamine, ascorbic acid, and L-arginine, fast and accurate response, and most importantly it is portable and inexpensive compared to other existing biosensor. Besides that, it also offers advantages of wide linear response range and good stability and reproducibility.

To the extent of our knowledge, there is little research focused on the G-Nf hybrid materials for the electrochemical detection of NO with a lowest detection limit. In this present work, a novel nanosized graphene-nafion (G-Nf) hybrid was employed as a sensing electrode material in an electrochemical sensor to study its sensitivity and selectivity toward NO. The electrochemical signal obtained from the NO sensor could be optimized by controlling the loading volume of the material on the electrode surface. The interference of ascorbic acid (AA) and dopamine (DA) during the determination of NO was also studied.

2. Experimental Section

2.1. Materials and Instruments

Graphite flakes was received from Asbury Graphite Mills, Inc. Sulfuric acid (H_2SO_4), phosphoric acid (H_3PO_4), hydrochloric acid (HCl), 3-Hydroxytyraminium chloride and L(+)-ascorbic acid were purchased from Merck. Potassium permanganate ($KMnO_4$) was purchased from R&M Chemicals. Nafion (200 mesh) was purchased from Ion Power Inc. Hydrogen peroxide (H_2O_2), ethanol, sodium phosphate monobasic (NaH_2PO_4), disodium phosphate dihydrate ($Na_2HPO_4.2H_2O$), and sodium nitrite ($NaNO_2$) were purchased from Sigma-Aldrich. All other chemicals used here were analytical grade and used without further purification. Photoluminescence (PL) measurements of the samples were recorded using a Renishaw inVia Raman microscope with an argon ion laser as the excitation source (325 nm).

The surface morphologies of the prepared materials embedded on the surface of GCE were analyzed using an Agilent-5100 atomic force microscope (AFM) in AC mode.

2.2. Synthesis of nanosized graphene-nafion (G-Nf) hybrid

The graphene oxide (GO) was prepared using a simplified Hummers' method [16]. A 50 mL of GO solution (0.5 mg/mL) was prepared by sonication using a horn type sonicator for 30 min. Meanwhile, a nafion (Nf) solution was prepared by dissolving Nf powder in an ethanol:water (1:1 *v/v*) mixture. And then, 10 mL of the Nf solution was added to 10 mL of the sonicated GO solution, and this mixture was subject to ultrasonication process for 30 min. Finally, the mixture was transferred into a Teflon-lined stainless-steel autoclave and heated at 180 °C. Three samples with different hydrothermal reaction times (8, 16 and 24 h) were prepared and labeled as G-Nf (8 h), G-Nf (16 h), and G-Nf (24 h).

2.3. Fabrication of G-Nf modified glassy carbon (GC/G-Nf) electrode

A GC/G-Nf electrode was fabricated by drop-casting 5 μL of the G-Nf solution on a pretreated GC electrode surface and allowing it to dry at 60 °C for 5 min. The electrochemical experiments were performed with a VersaSTAT 3 by Princeton Applied Research using a conventional three-electrode system. The GC/G-Nf electrode was used as a working electrode, a platinum wire served as a counter electrode, and Ag/AgCl was used as a reference electrode. A 0.1 M PBS with pH 2.5 was used as the electrolyte.

3. Results and Discussion

3.1. Characterization of G-Nf hybrids materials

As shown in **Fig. 1(a)**, the PL spectra for an aqueous solution of GO possess a broad emission peak at around 590 nm on excitation wavelength of 325 nm. The emission peak at

longer wavelength is a result of significant number of disorder-induced defect state within $\pi \rightarrow \pi^*$ transition possess by GO [17]. After hydrothermal process, the PL spectra of all three G-Nf hybrids were blue shifted to 416 nm as shown in **Fig. 1(b)**. This results demonstrated that the number of sp^2 clusters in reduced GO has increased, hence proving the successful of reduction process. Moreover, the position of this emission peak is similar as previously reported by Liu et al. which indicate the formation of graphene quantum dots [18]. The increases in degree of reduction of GO result in more shifted toward shorter wavelength due to the increase number of sp^2 cluster [17]. Therefore, G-Nf (16 h) has the highest degree of reduction as its peak shifting to the shortest wavelength. Besides that, one can find that the intensity of PL spectra decrease in order of: G-Nf (24 h) > G-Nf (8 h) > G-Nf (16 h). The PL emission is the result of the recombination of excited electrons and holes. Thus, the recombination rate of electrons and holes will affect the PL intensity. In general, a lower recombination rate for photogenerated electron and hole pairs will result in a lower PL intensity, and thus possess higher photocatalytic activity [19, 20]. Therefore, the G-Nf (16 h) hybrid is believed to shows great sensing performance due to high photocatalytic activity.

The morphological characterization and thickness measurements of the G-Nf hybrids embedded on the surface of GCE were carried out using AFM. **Fig. 2(a)** shows the AFM topographic image and depth profile obtained from a selected area of the G-Nf (8 h) hybrid having a lateral dimension of ~18 nm. The G-Nf hybrid with 16 h of hydrothermal treatment showed a good dispersion of nano-sized graphene into the Nf matrix (**Fig. 2(b)**). The average roughness of this sample was estimated to be about 8 nm in height based on the profiling depth measurement in the selected area of the film. When the hydrothermal treatment time was increased to 24 h, a high density for the agglomerated G-Nf hybrid on the surface of modified electrode was obtained with a height of up to 20 nm (**Fig. 2(c)**). The surface

roughness values of the G-Nf hybrids obtained after hydrothermal treatment period of 8, 16, and 24 h are shown in **Fig. 3**.

Fig. 3 presents AFM phase contrast images of the G-Nf hybrids (top row), along with three-dimensional views of the same surfaces (bottom row). The heights of the samples are represented by different color codes from dark to bright, which show the rough surfaces of the obtained G-Nf hybrids. The G-Nf (8 h) appeared to be built up from a few larger flakes of graphene that stacked together to form thicker flakes, as visualized by **Fig. 3(a)**. The stacking of a few graphene sheets might cause an increase in the thickness of the sample. As the hydrothermal processing time increases to 16 h, the G-Nf hybrid appears to be highly uniform with a smaller size and height compared to the G-Nf (8 h) hybrid (**Fig. 3(b)**). In addition, the 3D view reveals a good smoothness on the surface, which demonstrates a uniform distribution. However, after 24 h of hydrothermal treatment, the nanosized graphene tended to combine together and form agglomerations which then led to an increase in thickness of the surface roughness, as shown in **Fig. 3(c)**.

3.2. Electrocatalytic oxidation of NO at GC/G-Nf electrodes

It is well known that sodium nitrite ($NaNO_2$) serves as a source of NO by undergoing a disproportionation reaction (1) in an acidic solution (pH < 4) [21]. Hence, $NaNO_2$ was used as a precursor to produce NO in solution during the electrochemical study. The concentration of NO was determined by controlling the concentration of the injected $NaNO_2$ [22, 23].

$$[3\,HONO \rightarrow 2\,NO + H^+ + NO_3^- + H_2O] \quad (1)$$

Cyclic voltammograms were recorded using a 1 mM NO solution in 0.1 M PBS (pH 2.5) at a scan rate of 50 mV/s, and are shown in **Fig. 4**. The modified electrode did not show

any voltammetric response in the blank PBS solution, as can be seen in **Fig. 4(a)**. Upon the addition of the 1 mM NO in the PBS solution, an anodic peak potential at 0.85 V which can be related to the direct oxidation of NO can only be observed on the GC/G-Nf modified electrode. Upon hydrothermal treatment the GO is reduced to form RGO in the G-Nf hybrid. It is known from the literature, the RGO have better conductivity and electrocatalytic activity than the GO. Hence the hydrothermally prepared G-Nf hybrid (in RGO form) showed better electrocatalytic activity thereby increase the current response towards NO oxidation than the other electrode. Moreover, the synergic effect results from the hybridization of nanosized graphene and nafion facilitates the electron-transfer processes between the electrolyte and the GCE, thus increases the current respond. It was found that the current response toward the NO oxidation was higher for the GC/G-Nf (16 h) compared to the bare GC electrode and other modified electrodes (**Fig. 4(b)**). This result indicates a high electrocatalytic activity of GC/G-Nf (16 h) toward the oxidation of NO. Moreover, this result also revealed that the high degree of reduction and low defectiveness of the G-Nf (16 h) nanocomposite may lead to a high current response for NO oxidation. Hence, this GC/G-Nf (16 h) was chosen as a sensor electrode for the sensitive and selective detection of NO. The effects of different concentrations of NO on the current response of the GC/G-Nf (16 h) electrode were evaluated by CV, as shown in **Fig. 5**. It is obvious that the anodic peak current increased with an increase in the NO concentration.

The schematic view of the process of the detection of NO is given in **Scheme 1** and the possible reaction involved is shown in equation (2)[24].

$$NO \rightarrow NO^{+} + e^{-} \qquad (2)$$

It is suggested that the G-Nf acted as an electrocatalyt for the oxidation of NO to form nitrosonium ion (NO^{+}) during the electrocalytic process[25]. The GC/G-Nf modified electrode

exhibited high electrocatalytic activity towards NO oxidation, which enhances the electron transfer kinetics and improved the performance for detecting NO.

3.3. Electrochemical behavior of GC/G-Nf (16 h) electrode

The influence of the scan rate on the oxidation peak potential (E_{pa}) and peak current for NO at the GC/G-Nf(16 h) electrode in 0.1-M PBS (pH 2.5) were studied using CV, as shown in **Fig 6**. The current responses were found to be increased with an increase in the scan rate from 10 to 500 mV/s (**Fig. 6(a)**). The linear relation between the anodic peak currents and the square root of the scan rate is shown in **Fig. 6(b)**. As can be seen, the anodic peak current (I_{pa}) for the 1 mM NO varied linearly with the square root of the scan rate ($\nu^{1/2}$), with a linear regression equation of I_{pa} (μA) = 2.221 $\nu^{1/2}$ + 8.045 and a correlation coefficient R^2 = 0.986. This result indicates that the electron transfer of the GC/G-Nf (16 h) electrode is mainly controlled by a diffusion-controlled electrochemical process[25]. The diffusion coefficient was obtained according to the Randles–Sevcik equation, as shown in (3):

$$I_p = 0.4463\, nFAC\, (\frac{nF\nu D}{RT})^{1/2} \quad (3)$$

where n is the number of electrons transferred, F is the Faraday constant, A is the electrode surface area in cm^2, *v* is the scan rate in V/s, R is the gas constant, T is the temperature, D is the diffusion coefficient, and C is the analyte concentration in mol/cm^3. Using the above equation, the diffusion coefficient was calculated and gives a value of 8.51×10^{-7} cm^2 s^{-1}.

3.4. Influence of G-Nf loading on electrocatalytic performance

The influence of the G-Nf loading amount on the electrocatalytic oxidation performance was investigated and is shown in **Fig. 7(a)**. **Fig. 7(b)** displays the relation between the current response after the injection of 1 mM NO and the loading amount of the G-Nf (16 h) hybrid. It can be seen that the current response increases when the volume of G-

Nf (16 h) increases from 1 to 5 μL. The current response started to decrease after more than 5 μL was used to modify the GC electrode. This may have been due to the limited mass transport of the NO inside a thicker layer of G-Nf (16 h) formed on the surface of the GC electrode. Hence, 5 μL of G-Nf (16 h) was chosen to modify the GC electrode.

3.5. SWV detection of NO at GC/G-Nf (16 h) electrode

The sensitivity and selectivity of the sensor under the optimized detection conditions were tested, and a series of square wave voltammetry (SWV) curves were recorded with different NO concentrations at the GC/G-Nf (16 h) electrode, as shown in **Fig. 8(a)**. It could be observed that the anodic peak current increased linearly with an increase in the concentration of NO in the range of 0.05–0.45 mM, with a linear regression equation of I_{pa} = 0.062 M + 11.71 μ (R^2 = 0.998) (**Fig. 8(b)**). The limit of detection and sensitivity were calculated at a signal-to-noise ratio of 3 and gave values of 11.61 μM and 62 μA mM^{-1}, respectively. The sensitivity is determined from slope of the calibration figure. The very low detection limit observed can be ascribed to the effectively attached and well distributed G-Nf (16 h) hybrid on the surface of the GC electrode, which provided a larger surface area with better contact on the electrode surface. These result in an increase in the electron transfer reaction rate at the electrode–solution interface. In addition, the high degree of reduction and low defectiveness of the G-Nf (16 h) helps to increase the electrocatalytic activity, thus improving the sensing performance. The comparison of analytical parameters of present sensor electrode with some reported sensor electrodes for NO were showed in **Table 1**.

Table 1: Comparison of analytical parameters of some sensor electrode for NO determination.

Sensor Electrode	Fabrication method	Detection Method	Linear range (M)	Detection limit (M)	Ref.
nano-TiO_2 /Nafion film/GC	-	DPV	3.6×10^{-7} – 5.4×10^{-5}	$5.4 \cdot 10^{-8}$	26
PEI/[(PSS/PAH)$_2$/PSS/AuNP]^3	Infiltration, layer by layer	CV	0.05×10^{-3} – 0.5×10^{-3}	0.010×10^{-3}	27
hemoglobin–DNA/PG	Deposition	DPV	0.1×10^{-3} – 1×10^{-3}	1.8×10^{-5}	28
GC/G-Nf	Hydrothermal	SWV	0.05×10^{-3} – 0.45×10^{-3}	11.61×10^{-6}	This work

PEI/[(PSS/PAH)$_2$/PSS/AuNP]^3 = poly-(ethylenimine)/[(poly(sodium 4-styrenesulfonate)/,poly(allylamine hydrochloride))$_2$/ poly(sodium 4-styrenesulfonate)/gold nanoparticles]^3, PG = pyrolytic graphite,

3.6. Interferences studies

To verify the selectivity of the GC/G-Nf (16 h) electrode toward NO, the current response toward a ternary mixture containing 5 mM AA, 50 µM DA, and 5 mM NO was investigated using linear sweep voltammetry (LSV). As shown in **Fig. 9**, the anodic peaks of all three analytes are well resolved at the GC/G-Nf (16 h) electrode, with peak potentials at -0.02, 2.0, and 0.85 V, respectively, for AA, DA, and NO. These observations suggest that the GC/G-Nf (16 h) electrode had a good selectivity toward NO, and the simultaneous determinations of AA, DA, and NO could be possible in a real sample because the anodic peaks of these analytes are well separated.

4. Conclusions

A new, simple, and low-cost electrochemical sensor for NO based on a GC/G-Nf electrode was developed. A comparative study on the sensing responses to NO of G-Nf hybrids synthesized using different hydrothermal processing times was reported in this paper. We demonstrated the benefits of using G-Nf as the active material for NO sensing after the material undergoes 16 h of hydrothermal processing. The developed NO sensor showed a

lower detection limit of 11.61 μM, with a linear range of 0.05–0.45 mM and a higher sensitivity of 62 μA mM^{-1}. The lower detection limit for NO at the GC/G-Nf (16 h) electrode seemed to result from the high degree of reduction and low defectiveness of G-Nf (16 h), which helped to increase the electrocatalytic activity, and thus improved the sensing performance. This modified electrode also allowed the simultaneous selective detections of NO, AA, and DA. The results indicate that the proposed modified electrode has great potential to be applied as a sensor for NO detection in real sample analysis.

Acknowledgments

The authors gratefully acknowledge the UMRG Program Grant (RP007C/13AFR) by the University of Malaya and the High Impact Research Grant from the Ministry of Higher Education of Malaysia (UM.C/625/1/HIR/MOHE/SC/05).

Conflicts of Interest

The authors declare no conflict of interest.

References:

1. D. S. Bredt and S. H. Snyder, *Neuron*, 1992, 8, 3-11.
2. A. L. Burnett, *The Journal of Urology*, 1997, 157, 320-324.
3. A. Petros, D. Bennett and P. Vallance, *The Lancet*, 1991, 338, 1557-1558.
4. C. Napoli and L. J. Ignarro, *Nitric oxide*, 2001, 5, 88-97.
5. A. Mulchandani, C.-L. Wang and H. H. Weetall, *Analytical Chemistry*, 1995, 67, 94-100.
6. A. Mulchandani and C. L. Wang, *Electroanalysis*, 1996, 8, 414-419.
7. J. Yin, X. Qi, L. Yang, G. Hao, J. Li and J. Zhong, *Electrochimica Acta*, 2011, 56, 3884-3889.
8. B. Shah, T. Lafleur and A. Chen, *Faraday Discussions*, 2013, 164, 135-146.
9. X. Li, Y. Zhu, W. Cai, M. Borysiak, B. Han, D. Chen, R. D. Piner, L. Colombo and R. S. Ruoff, *Nano letters*, 2009, 9, 4359-4363.
10. Y. Wang, Y. Wan and D. Zhang, *Electrochemistry Communications*, 2010, 12, 187-190.
11. A. Reina, X. Jia, J. Ho, D. Nezich, H. Son, V. Bulovic, M. S. Dresselhaus and J. Kong, *Nano letters*, 2008, 9, 30-35.

12. J. S. Beckman and K. A. Congert, *Methods*, 1995, 7, 35-39.
13. Å. Wennmalm, B. Lanne and A.-S. Petersson, *Analytical biochemistry*, 1990, 187, 359-363.
14. P. Kuppusamy, P. Wang, A. Samouilov and J. L. Zweier, *Magnetic resonance in medicine*, 1996, 36, 212-218.
15. J. L. Wallace and R. C. Woodman, *Methods*, 1995, 7, 55-58.
16. N. M. Huang, H. Lim, C. Chia, M. Yarmo and M. Muhamad, *International journal of nanomedicine*, 2011, 6, 3443.
17. C.-H. Chuang, Y.-F. Wang, Y.-C. Shao, Y.-C. Yeh, D.-Y. Wang, C.-W. Chen, J. Chiou, S. C. Ray, W. Pong and L. Zhang, *Scientific reports*, 2014, 4.
18. F. Liu, T. Tang, Q. Feng, M. Li, Y. Liu, N. Tang, W. Zhong and Y. Du, *Journal of Applied Physics*, 2014, 115, 164307.
19. S. Hu, A. Wang, X. Li, Y. Wang and H. Löwe, *Chemistry, an Asian journal*, 2010, 5, 1171.
20. C. H. Kim, B.-H. Kim and K. S. Yang, *Carbon*, 2012, 50, 2472-2481.
21. P. Tripatara, N. S. Patel, A. Webb, K. Rathod, F. M. Lecomte, E. Mazzon, S. Cuzzocrea, M. M. Yaqoob, A. Ahluwalia and C. Thiemermann, *Journal of the American Society of Nephrology*, 2007, 18, 570-580.
22. A. Sivanesan and S. A. John, *Electroanalysis*, 2010, 22, 639-644.
23. A. Pandikumar and R. Ramaraj, *Indian Journal of Chemistry-Part A InorganicPhysical Theoretical and Analytical*, 2011, 50, 1388.
24. C. M. Li, J. Zang, D. Zhan, W. Chen, C. Q. Sun, A. L. Teo, Y. Chua, V. Lee and S. Moochhala, *Electroanalysis*, 2006, 18, 713-718.
25. Y.-L. Wang and G.-C. Zhao, *International Journal of Electrochemistry*, 2011, 2011, 6.
26. Y. Wang, C. Li and S. Hu, *Journal of Solid State Electrochemistry*, 2006, 10, 383-388.
27. A. Yu, Z. Liang, J. Cho and F. Caruso, *Nano letters*, 2003, 3, 1203-1207.
28. C. Fan, G. Li, J. Zhu and D. Zhu, *Analytica Chimica Acta*, 2000, 423, 95-100.

Figures and caption

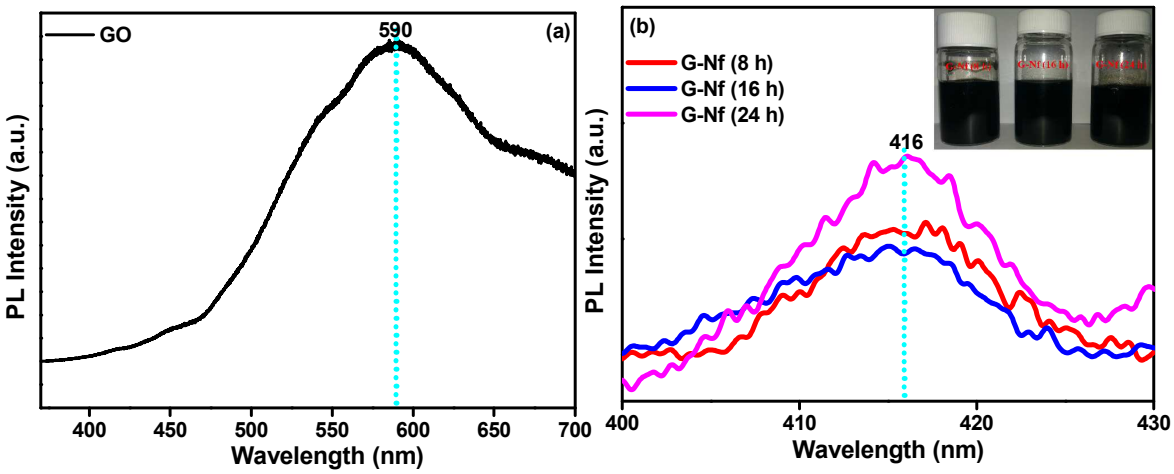

Fig. 1. PL spectra of **(a)** GO and **(b)** three different G-Nf hybrids.

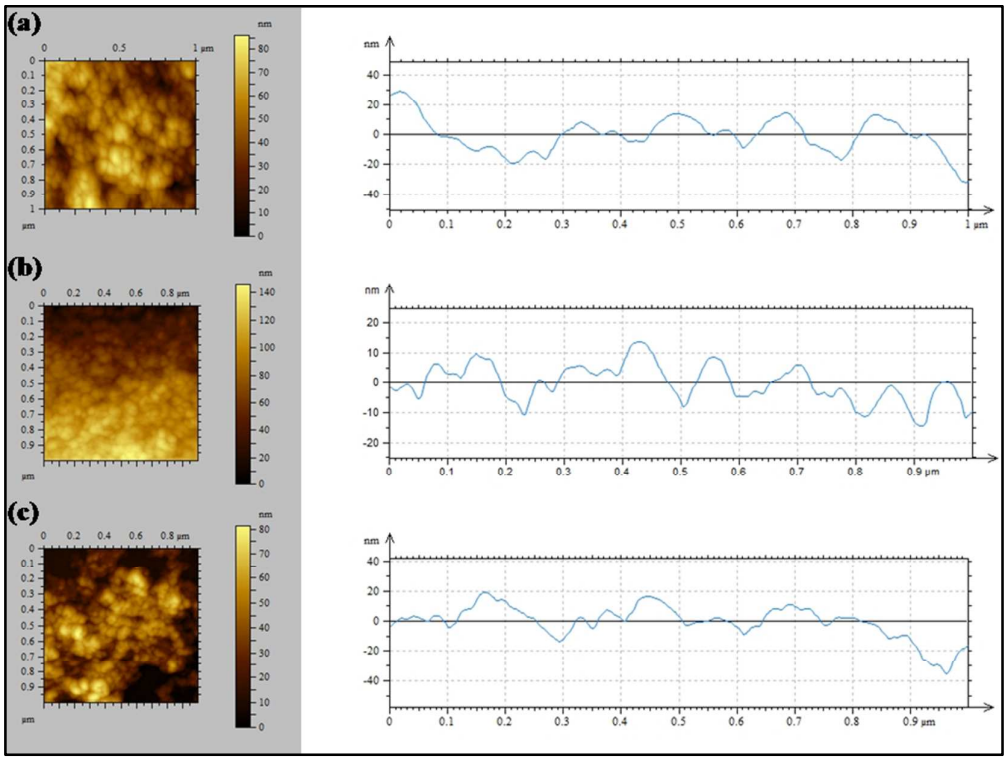

Fig. 2. AFM topographies of G-Nf hybrids obtained after hydrothermal treatment periods of **(a)** 8 h **(b)** 16 h, and **(c)** 24 h.

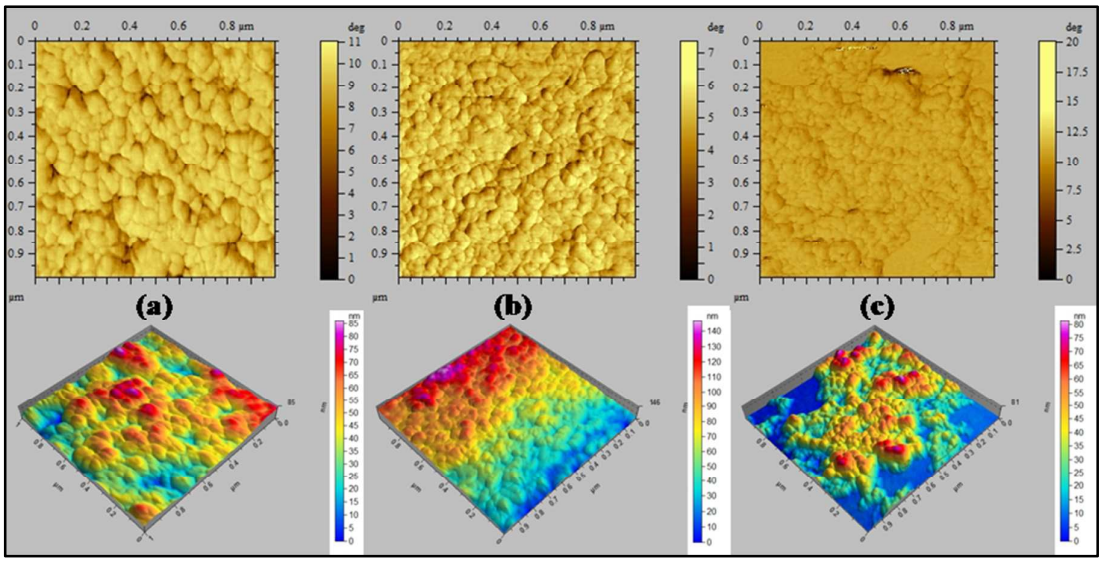

Fig. 3. AFM phases and 3D topographic images of G-Nf hybrids obtained after hydrothermal treatment periods of **(a)** 8 h **(b)** 16 h, and **(c)** 24 h.

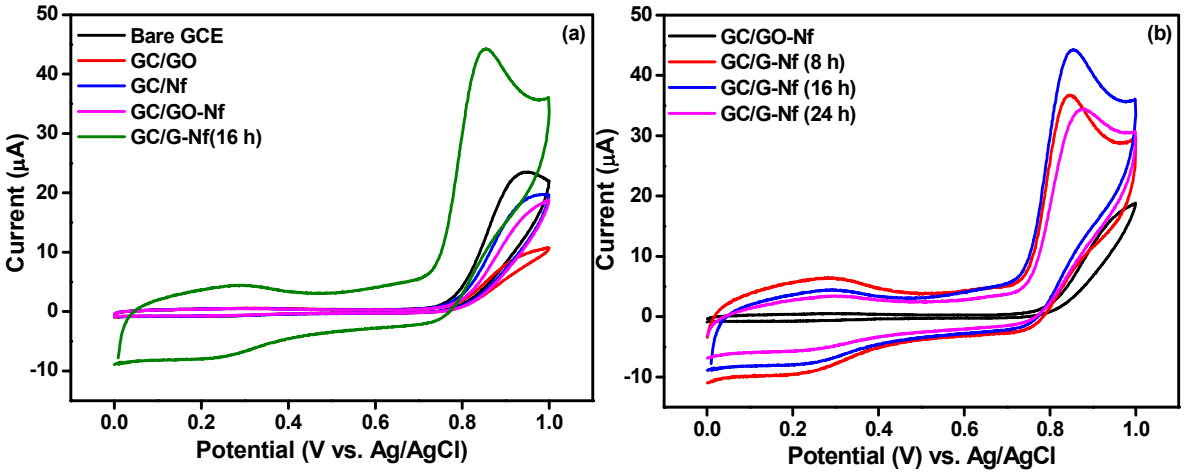

Fig. 4. (a) CV obtained for the bare GCE, GC/GO, GC/Nf, GC/GO-Nf and GC/G-Nf (16 h) electrodes in the presence of 0.1 M PBS (pH 2.5) containing 1 mM NO at scan rate of 50 mV/s. **(b)** CVobtained for the GC/GO-Nf, GC/G-Nf (8 h), GC/G-Nf (16 h) and GC/G-Nf (24

h) electrodes in the presence of 0.1 M PBS (pH 2.5) containing 1 mM NO at scan rate of 50 mV/s.

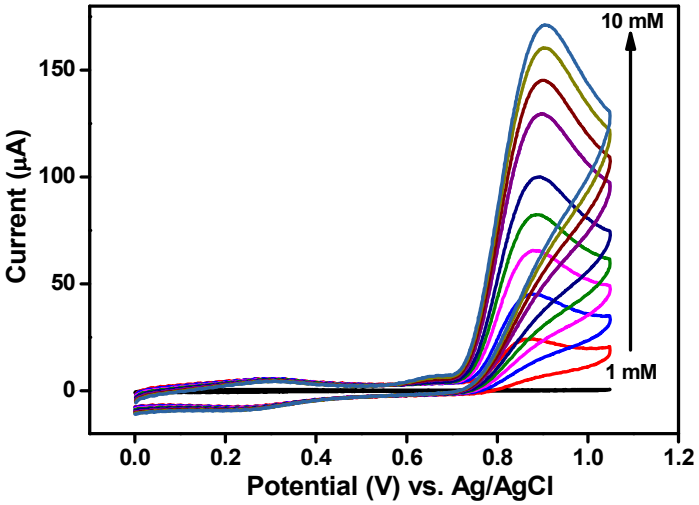

Fig. 5. CVs obtained for the GC/G-Nf (16 h) electrode in the presence of 0.1 M PBS (pH 2.5) and different concentration of NO (1 to 10 mM) at the scan rate of 50 mV/s.

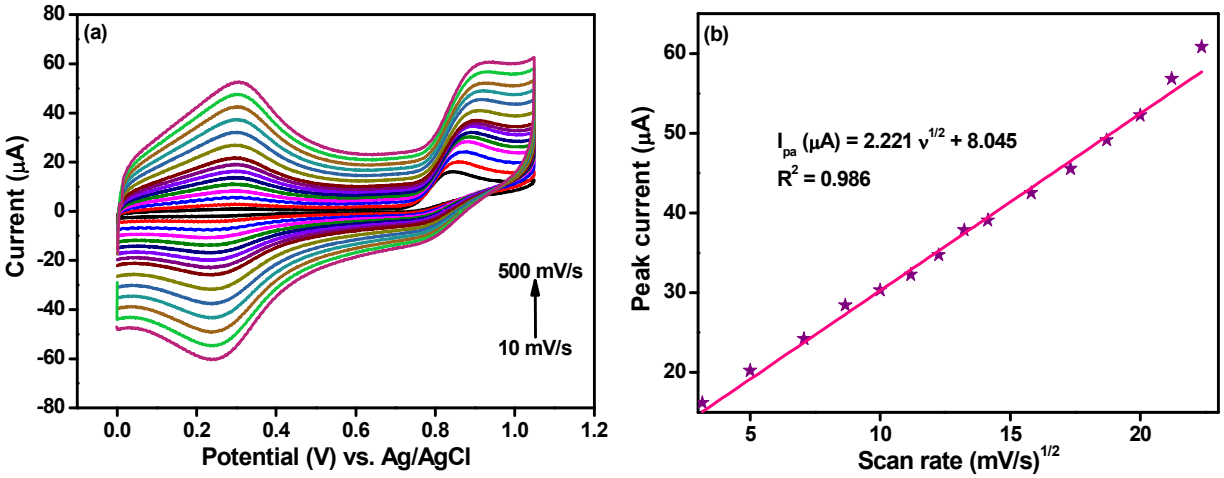

Fig. 6. (a) CVs obtained for the GC/G-Nf (16 h) electrode in the presence of 0.1 M PBS (pH = 2.5) containing 1 mM NO at different scan rates. **(b)** Plot of anodic peak current vs. square root of the scan rate obtained for the GC/G-Nf (16 h) electrode.

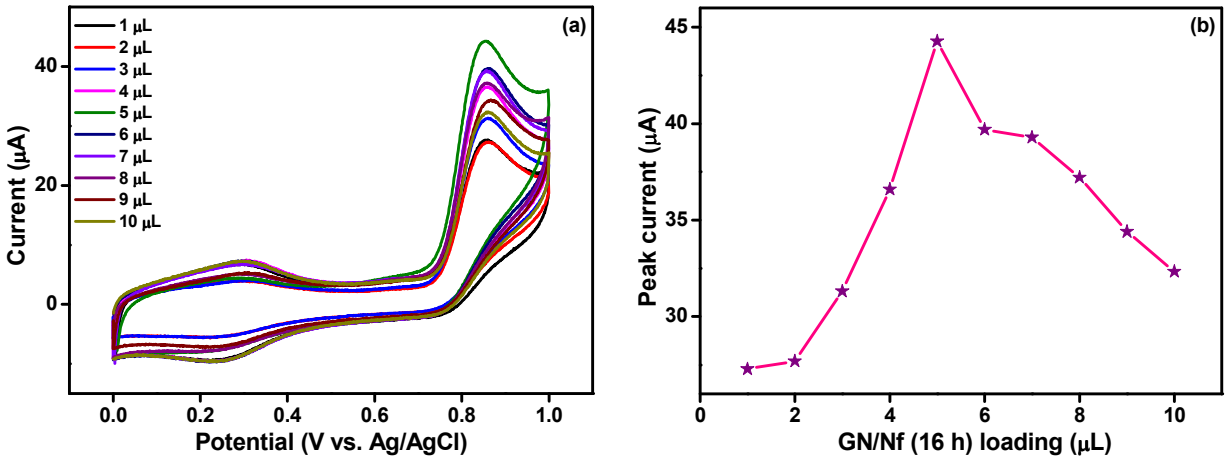

Fig. 7. (a) CVs obtained for GC/G-Nf (16 h) electrode with different amount of sample loading. **(b)** Plot of G-Nf (16 h) loading *vs.* anodic peak current response obtained for the 1mM NO in 0.1M PBS (pH 2.5) at scan rate of 50 mV/s.

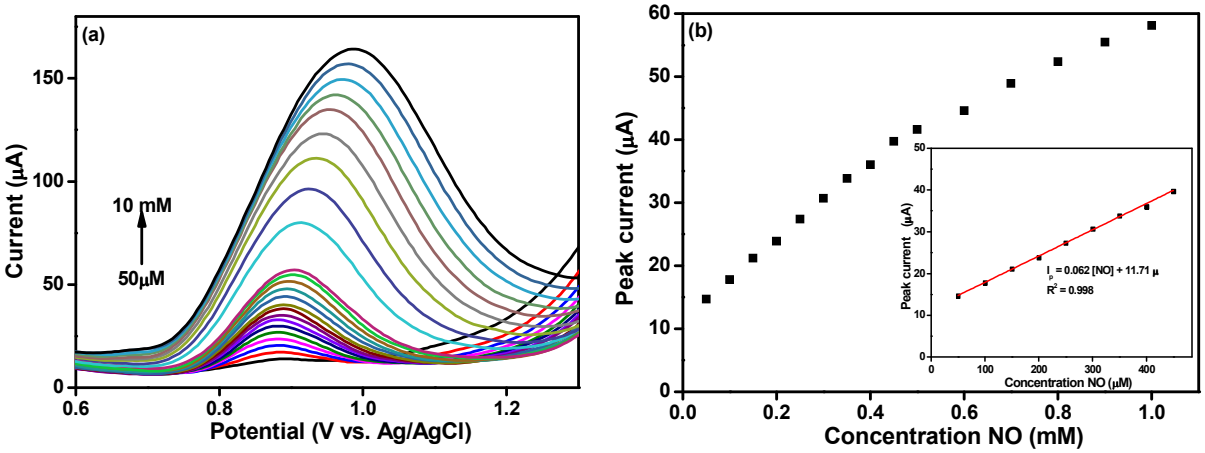

Fig. 8. (a) SWV obtained for GC/G-Nf (16 h) electrode in 0.1 M PBS pH 2.5 containing different concentration of NO (50 µM to 10 mM) at scan rate of 50 mV/s. **(b)** Correlation between the concentration of NO and peak current quantified from the SWV. **(b)** (**Inset**): Enlarged view of plot obtained for the peak current *vs.* concentration of NO at lower concentration level.

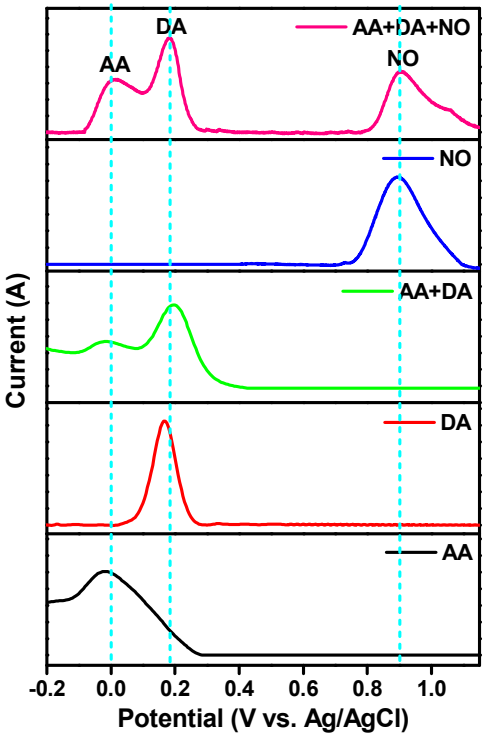

Fig. 9. LSV obtained for the GC/G-Nf (16 h) electrode in 0.1 M PBS (pH 2.5) with the mixture of 5 mM AA, 50 µM DA and 5 mM NO.

Facile Synthesis of Nanosized Graphene/Nafion Hybrid Materials and Its Application in Electrochemical Sensing of Nitric Oxide

Norazriena Yusoff [1], Alagarsamy Pandikumar [1], Marlinda Ab Rahman [1], Huang Nay Ming [1,*] and Lim Hong Ngee [2]

GRAPHICAL ABSTRACT